Nuclear Inst. and Methods in Physics Research, A xxx (xxxx) 165481

Contents lists available at ScienceDirect

Nuclear Inst. and Methods in Physics Research, A

journal homepage: www.elsevier.com/locate/nima

Fatigue analysis of the Spallation Neutron Source 2 MW target design

Justin Mach [a,*], Kevin Johns [a], Sarma Gorti [b], Hao Jiang [c]

[a] Neutron Technologies Division, Oak Ridge National Laboratory, Oak Ridge, TN, USA
[b] Computational Sciences and Engineering Division, Oak Ridge National Laboratory, Oak Ridge, TN, USA
[c] Materials Science and Technology Division, Oak Ridge National Laboratory, Oak Ridge, TN, USA

ARTICLE INFO

Keywords:
SNS
PPU
Spallation neutron source
Mercury target vessel
Fatigue
Weld fatigue

ABSTRACT

Upgrades to the Spallation Neutron Source (SNS) at Oak Ridge National Laboratory are under way with two major projects. The first project is the Proton Power Upgrade (PPU), which will double the power capacity of the SNS accelerator system to enable the operation of a future second neutron source target station—the second project. PPU also will increase power to the SNS first target station – which currently operates at 1.4 MW with 1.0 GeV protons – to 2 MW with 1.3 GeV protons. Final design of the PPU 2 MW target module is finished, including all necessary design and analysis calculations. The fatigue evaluation described herein is an assessment of the fitness of the PPU 2 MW target mercury vessel to resist failure from cyclic loading from the pulsed 60 Hz proton beam and thermal changes from disrupted operation. In addition to the reliability predictions, the method, detail, and depth of this fatigue evaluation are superior to those of past target design assessments. The thermal fatigue life is predicted to exceed 3125 thermal cycles per 1250 h of operation for all load cases. The design also meets the (relative) fatigue design goal for combined thermal and pulse loading of greater than 0.5 times the minimum fatigue life calculated for a jet-flow target design operating at 1.4 MW—the most robust design to date in terms of resistance to fatigue failure. From the onset of the PPU, it has been known that pulse loading requires effective application of helium gas injection into the target mercury to reduce beam pressure loading. For the PPU 2 MW target, none of the pulse load cases requires a maximum strain reduction from gas injection of more than 50% (for base material) to meet the fatigue design goal. This level of reduction is achievable from gas injection, according to historical strain measurements from 1.4 MW target operation. Overall, the PPU 2 MW target design is predicted to have superior resistance to fatigue failure compared with past target designs.

1. Introduction

The Spallation Neutron Source (SNS) at Oak Ridge National Laboratory (ORNL) produces neutrons for science experiments at the SNS First Target Station (FTS) [1] using a process called spallation, in which high-energy protons strike a high-atomic-number material. In the SNS case, liquid mercury flows through a 316L stainless steel vessel, which is a primary component of the target module assembly. Fig. 1 is an exploded view of the SNS target module; the mercury vessel is composed of the nose, inner window, front body, swirl bubbler, transition, insert, and manifold components, as well as the corresponding welded joints, gas supply, and other hardware. Fig. 2 shows a section view with the bulk mercury flow paths highlighted for the two outer supply flows (in blue) and the common inner return flow (in red).

The bolt-on-shroud, or BOS, (not shown) is a secondary vessel in the target module assembly that prevents mercury from escaping into the core vessel at the FTS in the event of a mercury vessel leak. The SNS design approach maintains structural independence between the BOS and mercury vessel. Therefore, the BOS is analyzed independently, and it is not discussed further in this paper.

The PPU project [2,3] will double the SNS accelerator power capability and send 2 MW of 1.3 GeV proton beam to the existing FTS mercury target module. The FTS currently operates with a 1.0 GeV proton beam at 1.4 MW. The PPU equates to an approximately 43% increase in power on target and a correspondingly higher-amplitude cyclic load-

☆ This manuscript has been authored by UT-Battelle LLC under contract DE-AC05-00OR22725 with the US Department of Energy (DOE). The US government retains and the publisher, by accepting the article for publication, acknowledges that the US government retains a nonexclusive, paid-up, irrevocable, worldwide license to publish or reproduce the published form of this manuscript, or allow others to do so, for US government purposes. DOE will provide public access to these results of federally sponsored research in accordance with the DOE Public Access Plan (http://energy.gov/downloads/doe-public-access-plan).

* Correspondence to: Oak Ridge National Laboratory, P.O. Box 2008, M.S. 6476, Oak Ridge, TN, 37831-6476, USA.
E-mail address: machjc@ornl.gov (J. Mach).

https://doi.org/10.1016/j.nima.2021.165481
Received 11 December 2020; Received in revised form 29 March 2021; Accepted 24 May 2021
0168-9002/© 2021

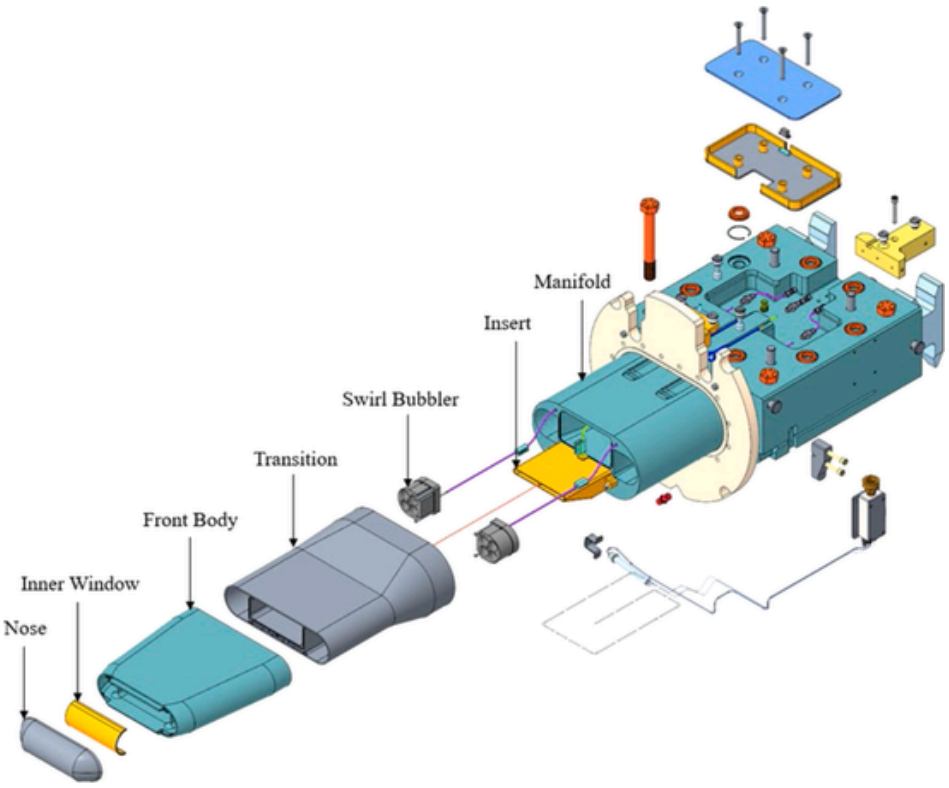

Fig. 1. Exploded view of the PPU 2 MW target module.

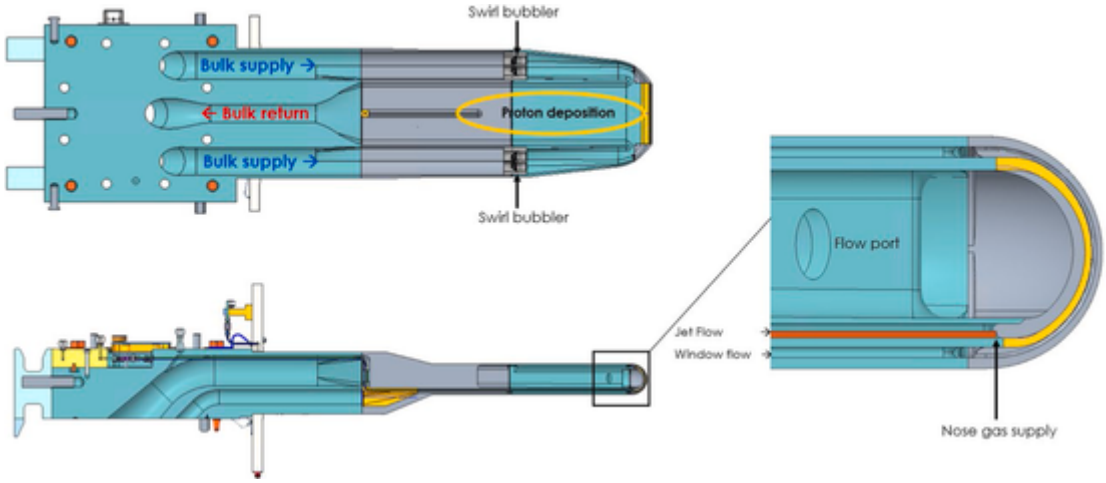

Fig. 2. Mercury target vessel section view with bulk mercury flow paths shown—two outer supply flows (blue) with one common inner return flow (red).. (For interpretation of the references to color in this figure legend, the reader is referred to the web version of this article.)

ing. The high-energy, short-duration (<1 μs) proton beam is pulsed at 60 Hz. Mercury and vessel heating is essentially isochoric, causing intense pressure waves [4] and mercury cavitation [5]. Cyclic loading of the vessel is complex, as it responds to pressure waves and operating temperature changes. The mercury flows through a heat exchanger, and the target module quickly reaches a steady operating temperature distribution over minutes; however, beam interruptions create a second source of thermal cyclic loading. A nominal operating year is planned for nearly 5000 h, with two or three target replacements planned each year proactively, rather than in response to a target leak. This approach is expensive but helps ensure reliable operation for neutron science users.

Two forms of cyclic loading are analyzed to calculate fatigue life. The frequency and number of thermal and mechanical cycles are vastly different but are superimposed during the operation of the target. The thermal cyclic loading – room temperature to operating temperature – is estimated at no more than 3125 transients in 1250 operating hours. This conservative estimate is based on operational experience at SNS. The pressure wave mechanical response occurs in a time span of milliseconds, and the target may experience up to 10^9 such pulse cycles in a lifetime.

The primary loading inputs to the structural and fatigue analyses come from accelerator physics, neutronics, and computational fluid dynamics (CFD) simulations, as shown in the left image of Fig. 3. The structural analyst then executes the workflow in the right image of Fig. 3, culminating in the fatigue analysis as described in this paper. The software used to perform the static and dynamic simulations are the 2019 versions of Abaqus/Standard and Abaqus/Explicit (© Dassault Systèmes),

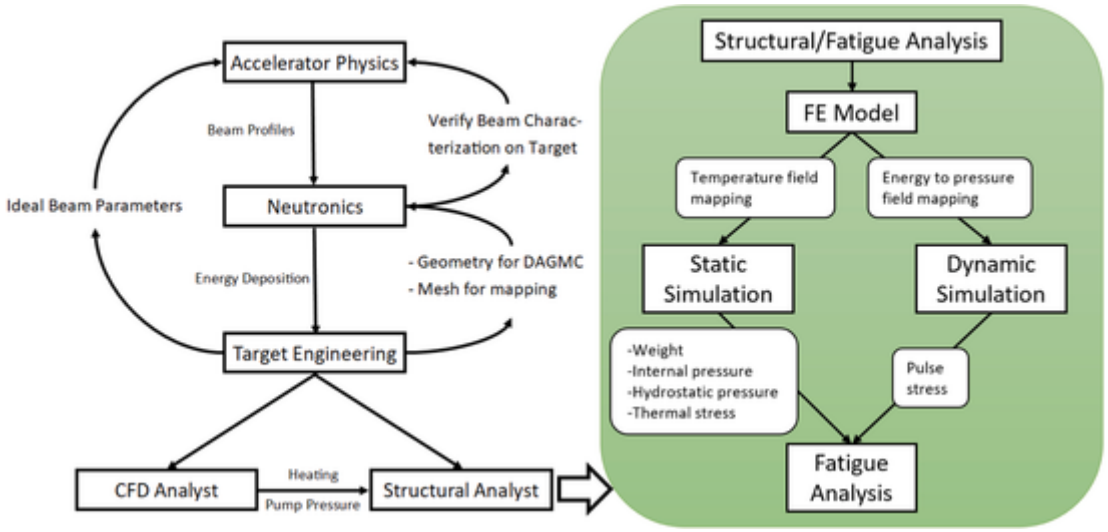

Fig. 3. High-level workflow to complete a target design structural and fatigue analysis. Components on the left provide input to the structural analyst to complete the workflow on the right.

respectively; and the software used to perform the base material fatigue analysis is the 2019 version of fe-safe™ (© Dassault Systèmes), which uses the fe-safe/Verity module for weld fatigue analysis.

2. Design criteria and fatigue design goals

The target structural design criteria are derived from the ASME Boiler and Pressure Vessel Code (BPVC), Section VIII, Division II, Part 5: Design by Analysis [6]. The target is not a safety-accredited device and is not code stamped. A functional requirement is that the PPU target should operate for at least 1250 h at a beam power of up to 2 MW. This lifetime goal equates to 2.7×10^8 pulses and corresponds to four planned target replacements per year, but fewer target changes are highly desirable. A limiting goal is to change the target when it reaches the administrative radiation damage limit, currently set at 12 dpa for the BOS, which corresponds to approximately one target change per year (for 5000 annual operating hours). The design specification states that no more than 3125 beam trips are expected in 1250 h. In summary, the PPU 2 MW target is required to endure

- 2.7×10^8 pulse cycles during 1250 h at a beam power of up to 2 MW (2500 MWh)
- 3125 beam trips (thermal cooling and heating cycles) per 1250 h

The ASME BPVC allowable stress amplitude (for base material) at a given life is conservative relative to published test data for conditions like those experienced by the 2 MW target, although the actual combination of conditions (radiation, mercury exposure, etc.) cannot be perfectly replicated in any available laboratory. In a similar manner, further evidence is provided here for using allowable stress amplitudes provided by the fatigue analysis software program fe-safe™ that are above those in the ASME BPVC for 316L stainless steel. Fig. 4 compares the ASME BPVC stress–life curve (allowable stress amplitude vs. cycles to failure) at room temperature to room temperature and high temperature curves from fe-safe™ and estimated curves from data published by Strizak et al. [7] and J-PARC (Japan Proton Accelerator Research Complex) [8].
Fatigue strength at the design lifetime of 2.7×10^8 pulse cycles is labeled on the plot for several of the curves. The ASME curve – a design basis curve with incorporated safety factors on stress and cycles – is conservative relative to all other curves (for 200 °C and below) at approximately 10^5 cycles and above, which is less than one half hour in a target lifetime. Therefore, we conclude that the ASME curve is conservative relative to all other curves in general for cyclic pulse loading. Conservative is defined here as a lower allowable stress amplitude for a given number of cycles to failure (or fatigue life). The fe-safe™ 200 °C curve is also conservative relative to the published (and interpolated) 200 °C data at approximately 1.5×10^6 cycles and above. The limit on the maximum wetted temperature of the mercury vessel is 200 °C, and it is known from historical analysis (and continues to be the case with the PPU target) that the predicted lowest life locations in a target for pulse loading are on the wetted surface. The fatigue life predictions for the PPU 2 MW target are $O(10^6)$ at the lowest life location in the base material. Therefore, we conclude that the fe-safe™ 200 °C and below temperature curves are conservative relative to the published data and they are a less conservative and more practical (for target design) substitute for the ASME BPVC curves. It is important to note that due to the low fatigue life predictions for pulse cyclic loading that are $O(10^6)$, the fatigue predictions are always treated as relative and compared with past target designs. Also, the ASME curve is less conservative than the fe-safe™ curves and experimental data at the low life values of $O(10^3–10^4)$, however, past thermal cyclic loading analyses that utilize the ASME criteria have typically shown life results at $O(10^5)$ and above where the ASME criteria are conservative.

The structural stress method in the fe-safe™/Verity module is used for weld fatigue analysis of the PPU 2 MW target. The steel weld S–N master curves in Verity are only meant to be used with the structural stress weld fatigue assessment method as described in Section 5.5.5 of ASME BPVC Sec. VIII Div. 2 or as implemented in a weld fatigue analysis software tool like Verity. The structural stress amplitude allowable for welds inherently includes geometrical and loading factors that multiply the stress amplitude that is directly calculated from nodal forces in the FEA results. The underlying data that these curves are based on originate from fatigue testing of welded samples that include the as-fabricated residual stress and stress concentrations associated with weldments of various geometries and welding processes.

Under-prediction of fatigue life has been typical for pulse cyclic loading on previous target designs. The reasons for the under-prediction include (but are not limited to) errors in the stress prediction models, conservatism in the fatigue curves, inaccuracy in the fatigue method (multi-axial and weld fatigue are active research areas), strain reduction effects from gas injection (not included in the analyses), interaction with cavitation damage/erosion, environmental effects such as irradiation and mercury exposure, and manufacturing effects such as surface treatment and finish. The “jet-flow” (JF) target (operating with gas injection) is the most robust target design used during SNS opera-

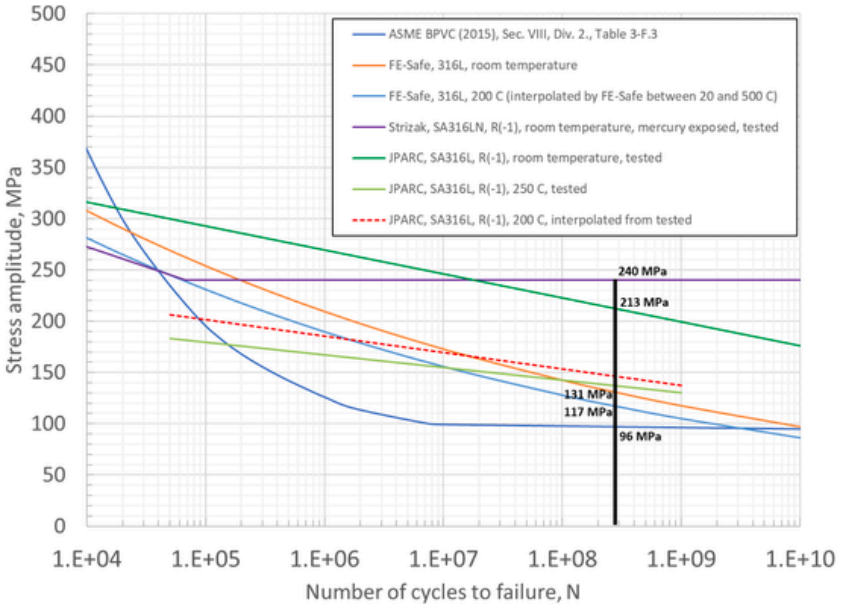

Fig. 4. Comparison of stress–life curves for 316L stainless steel from the ASME BPVC, the fe-safe™ software program, and estimated curves from published data by Strizak et al. [7] and J-PARC [8].

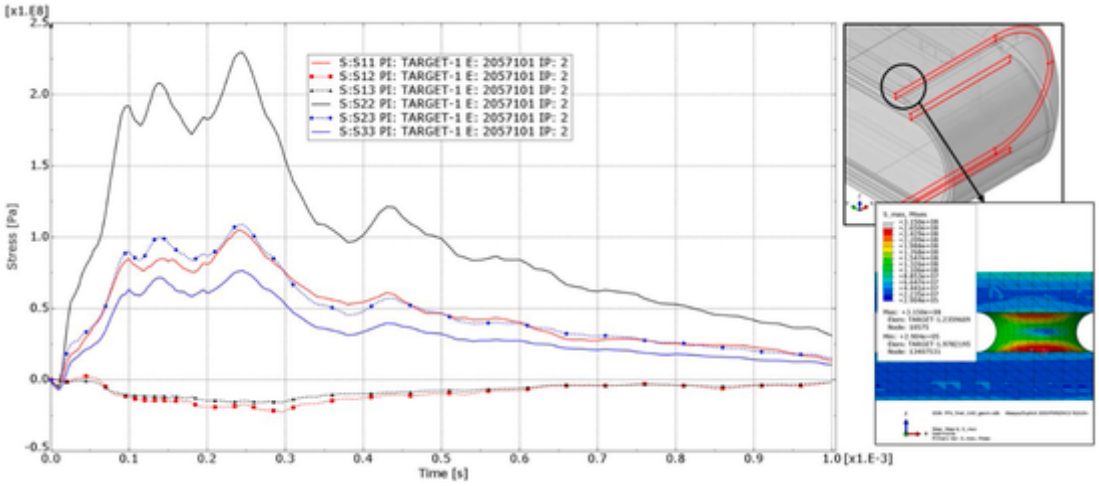

Fig. 5. Multi-axial, time-varying stress components due to pulse pressure wave at a highly stressed location in the front body of the PPU 2 MW target design.

tional history—operating for more than 2000 h at 1.4 MW. For these reasons, the fatigue design goals are defined as the following:

- For the base material, greater than 0.5 times the minimum combined thermal and pulse fatigue life of a JF target at 1.4 MW, and a required strain reduction from gas injection equal to or less than 50% to achieve 270M pulse cycles
- For the weld material, greater than 0.5 times the minimum combined thermal and pulse fatigue life of a JF target at 1.4 MW

3. Analysis model

The essentials of the explicit dynamic pulse simulation method are described by Riemer [9,10]. The stress time history from this model provides the cyclic pulse loading for the fatigue analysis described here. An example of the multi-axial, time-varying stress history due to the pulse pressure wave is shown in Fig. 5.

The static simulation provides the stress states due to self-weight (gravity), internal (mercury pump) pressure, hydrostatic pressure, and steady-state thermal loading. All these simulation models and corresponding stress analyses are detailed in a related paper that is in preparation, while the most important aspects of these models for fatigue analysis are discussed in this section.

3.1. Geometry and mesh

For conducting a combined thermal and pulse fatigue analysis, the corresponding static and dynamic models, respectively, must be based on the same model geometry (including spatial location and orientation) and an identical mesh, including node numbers and elements. The simulation model includes partitioned regions within the steel domain that represent the approximate geometry of the weld fusion zones. The locations of the seven welds that were analyzed are shown in a $\frac{1}{2}$ half symmetry model in Fig. 6, with close-up views included in Fig. 7. Table 1 summarizes the analyzed welds with classification by joint type, weld type, penetration, welding process, surface treatment, and drop-thru—where EB = Electron-beam, GTAW = Gas tungsten arc welding, and EDM = Electron-discharge machining. Based on the metallography of the front body to transition EB weld (as shown in Fig. 8),

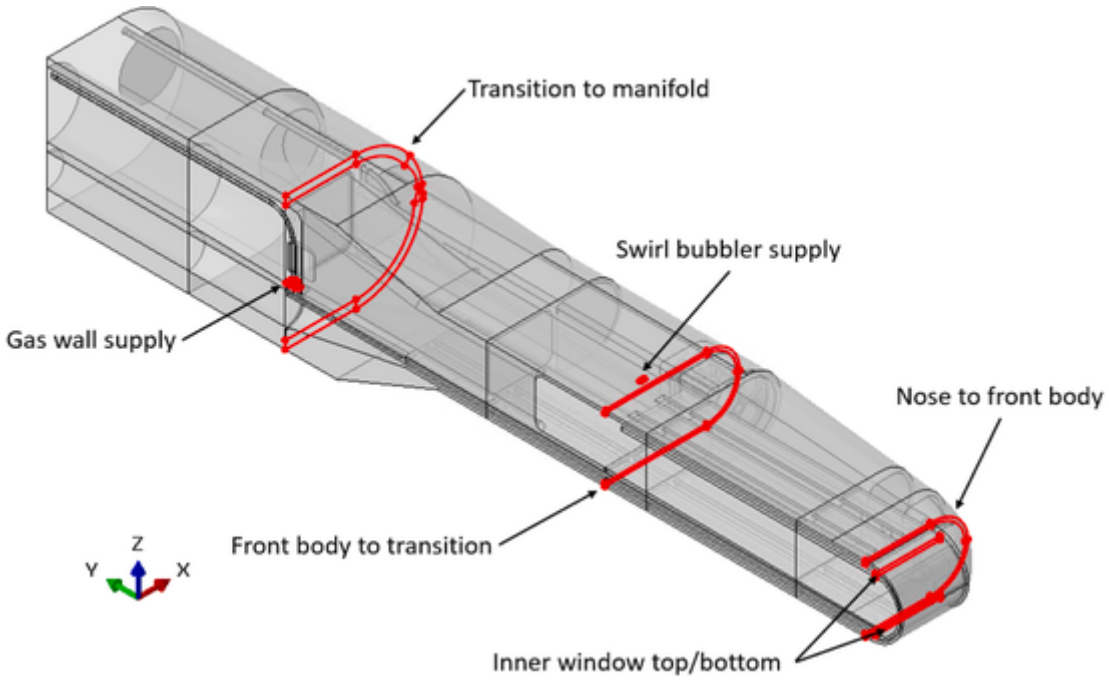

Fig. 6. Welds analyzed in the PPU 2 MW target.

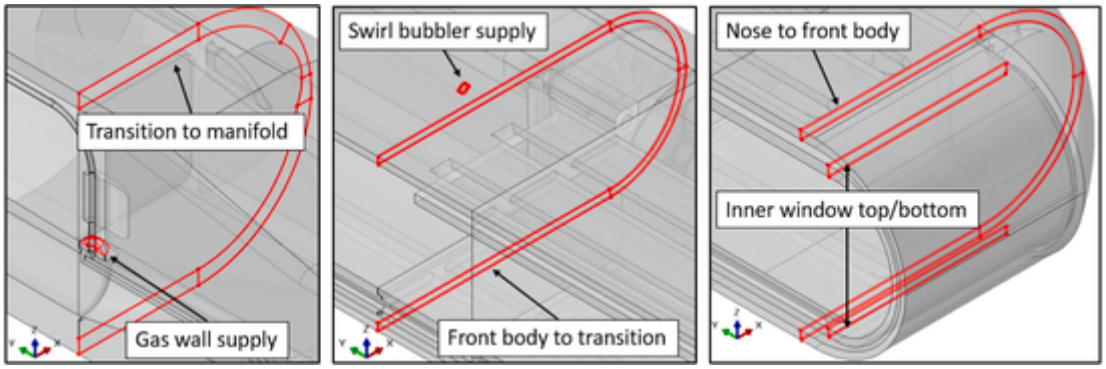

Fig. 7. Welds analyzed in the PPU 2 MW target (close-up views).

Table 1
Analyzed welds classified by joint type, weld type, penetration, welding process, surface treatment and drop-thru.

Weld	Joint type	Weld type	Penetration	Welding process	Surface treatment	Drop-thru	Inspection[b]
Front body to transition	Butt-joint	Square groove	Full	EB	GTAW with filler	50%–100% of weld length[a]	VT, PT, UT, RT
Nose to front body	Butt-joint	Square groove	Full	EB	Machine stock on outside	100% of weld length	VT, PT, UT, RT
Inner window top and bottom	Butt-joint	Square groove	Full	EB	Wire EDM drop-thru on inside	0% of weld length	VT, PT, UT, RT
Transition to manifold	Butt-joint	U-groove	Full and partial—varies along length	GTAW with filler	None	N/A	VT, PT, UT
Gas wall supply	T-joint	Fillet	None	GTAW with filler	None	N/A	VT, PT
Swirl bubbler supply	Butt-joint	Square groove	Full	Orbital, GTAW without filler	None	N/A	VT, PT

[a] Regions of weld root surrounding swirl bubblers may require post-machining for a proper fit.
[b] Inspection type: VT = visual, PT = dye penetrant, UT = ultrasonic, RT = radiographic.

the widths of the front body, nose, and inner window top/bottom welds are modeled as a constant 1 mm from the surface to the root.

The drop-thru geometry varies along the weld length, and it is difficult to represent in a model. The drop-thru (like the weld reinforcement at a weld toe) does not add strength to the butt joint weld, and the stress concentration it creates is detrimental to fatigue life. An accurate representation of the stress singularity at the weld root/toe is not required, because the stress linearization procedure used in the weld fatigue analysis method removes the peak stress from the fatigue life assessment [11]. However, the finite element model must accurately repre-

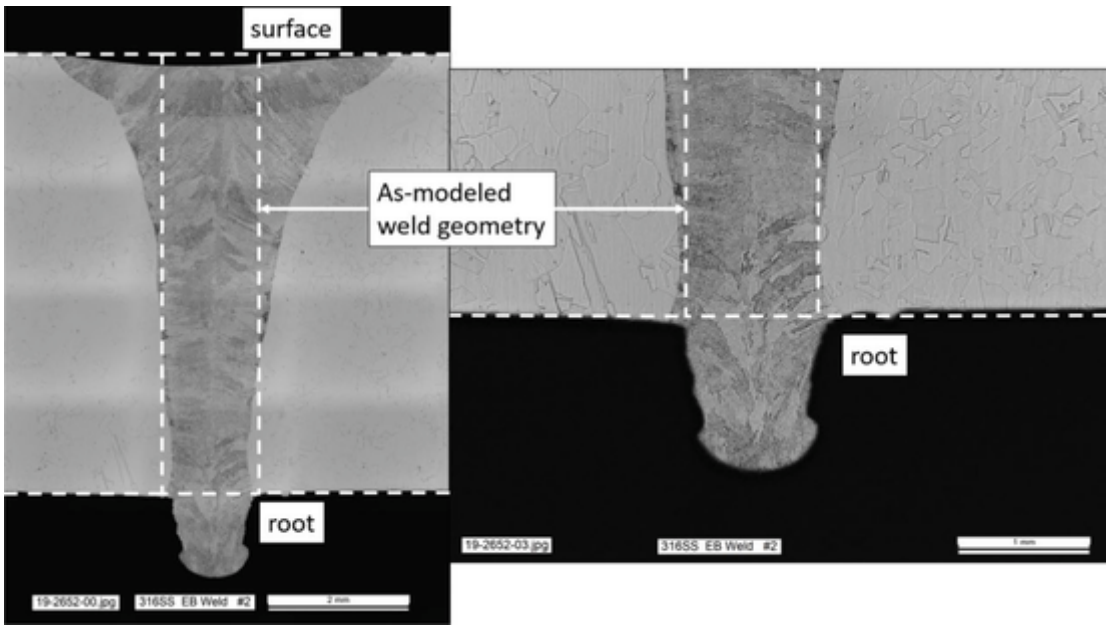

Fig. 8. Cross-section of an EB weld with drop-thru from the front body to the transition section of a target, with dashed box representing an as-modeled weld domain (images courtesy of D. McClintock, ORNL).

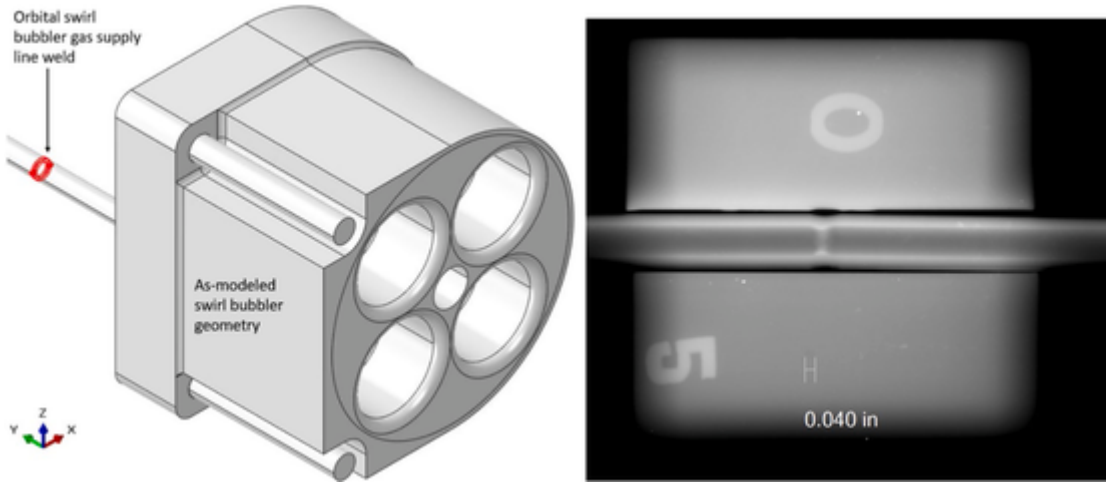

Fig. 9. Full-penetration orbital weld model in swirl bubbler gas supply line (left) and X-ray image (courtesy of E. Vidal, ORNL) showing the approximate width of the weld (right).

sent the membrane and bending stress across the weld failure plane, which is dictated by element choice and mesh refinement. The constant width simplifies the modeling and satisfies the requirement for a 3D meshed volume in the weld definitions. The EB welds with drop-thru are most likely to fail from the root, because the stress concentration is much greater at the root than at the surface (as shown at the top of the left image in Fig. 8); this image shows a cosmetic EB welding overpass to smooth the weld toe.

The swirl bubbler's function is to introduce helium gas bubbles into the mercury flow to reduce the impact of the pulse pressure wave and cavitation damage [12]. The PPU project incorporated a swirl bubbler design [13] like one that has been successfully deployed at J-PARC for several years [14]. The swirl bubbler supply weld is an orbital weld that joins a gas supply line to the swirl bubbler, as shown in the left image of Fig. 9. This weld is also modeled as a constant 1 mm width, based on a measurement of a manufacturing test article (shown in the right image of Fig. 9).

The transition weld is modeled in the same manner as the other main body welds, except that the width is 0.5 mm. This is simply a modeling convenience based on the gap remaining in the model that represents the partial penetration of this weld along most of its length. This weld is the least susceptible (of the main body welds) to fatigue failure because of its location toward the rear of the target. Finally, the gas wall supply fillet weld has equal leg lengths of 5/16 inch; it functions as a seal between a supply line and the target body, as shown in Fig. 10. The potential failure paths along the toe, root, throat, and fusion regions are highlighted.

The weld meshing follows the same practice as the static and dynamic finite element analysis (FEA) simulations. The element type is a 10-node, second order tetrahedron for all models. All welds have two or more elements along the weld thickness direction, and the surface meshes are mapped if possible. All groove welds have one element through the width to prevent element size, transition, and quality issues; this is the minimum required to analyze the fusion failure mode, which was deemed the most appropriate mode for these weld types. The surfaces of the weld meshes, as viewed from the front of the target in the beam travel direction, are shown in Fig. 11.

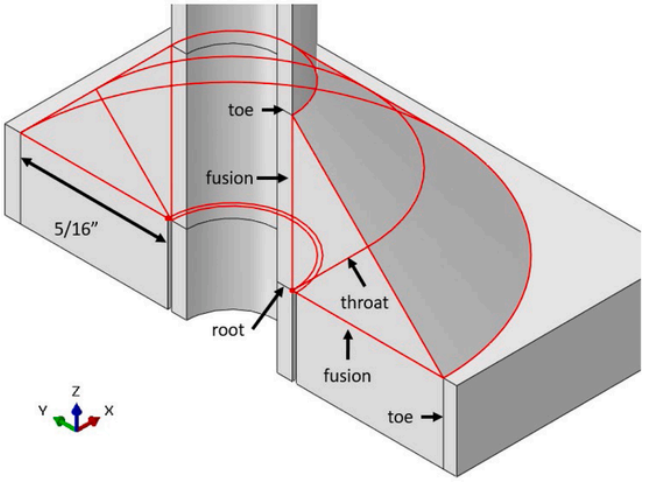

Fig. 10. Potential failure paths of gas wall supply fillet weld to target body.

3.2. Loading

Table 2 shows the load cases considered in the fatigue analysis, which primarily consist of shifts in the beam position or focus, and changes in the mercury pump speed. The reduced-pump-speed cases lower the internal pressure and reduce heat removal, which causes higher thermal stresses. The GL case refers to a hypothesized gas layer condition at the top of the return flow in the target, leading to an increase in temperature and thermal stress in this region.

3.3. Output

The stress results from the static and dynamic FEA simulations are needed for the base material fatigue analysis. The stress due to weight and pressure loads only, and the stress due to thermal load only, are input from the static model; and the stresses from 140 frames of output over 0.001 s of simulation duration are input from the dynamic model. The dynamic simulation output frames are more finely spaced toward the beginning of the simulation to capture the rapid change in the stress state (cf. Fig. 5). The weld fatigue analysis requires the element nodal forces output in the weld regions.

4. Analysis methods

Fig. 12 shows the high-level fatigue analysis workflow with settings and inputs that are described in more detail in the following sections.

The base material analysis is performed on the surface nodes only, which contain the highest stresses that drive fatigue damage, and it is computationally more efficient. The weld fatigue analysis of the butt joint welds focuses on fatigue failure along the fusion planes—the interface between the weld fusion zone and the base material, i.e., the heat-affected zone. The fatigue life is evaluated on both fusion planes and from the outer surface "toe" of the weld and the inner surface "root" of the weld (cf. Fig. 8). The minimum fatigue life at these four potential fatigue crack initiation locations is taken as the predicted fatigue life for that weld. The weld fatigue analysis of the fillet-type weld has more potential failure paths than the butt joint welds, as shown in Fig. 10. All of these potential failure paths are analyzed from both directions and the

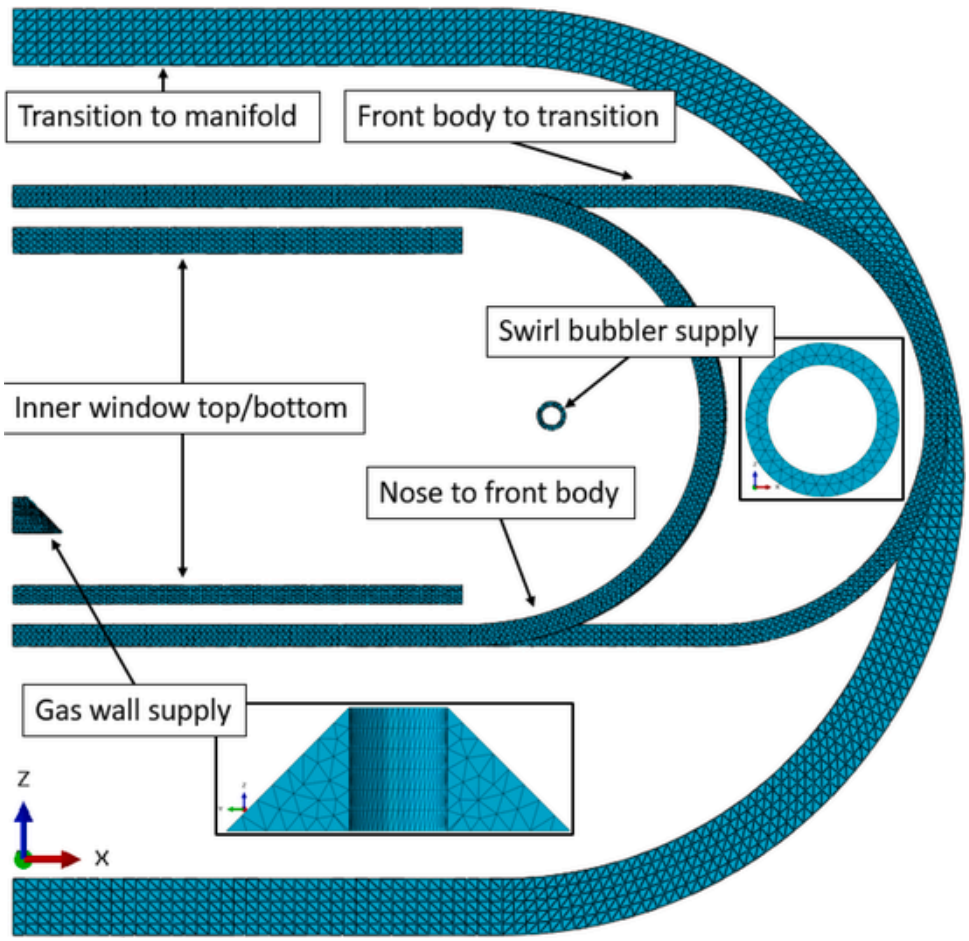

Fig. 11. Finite element meshes for all analyzed welds, as viewed from the front of the target in the direction of the beam (except as oriented in the close-up image of the gas wall supply).

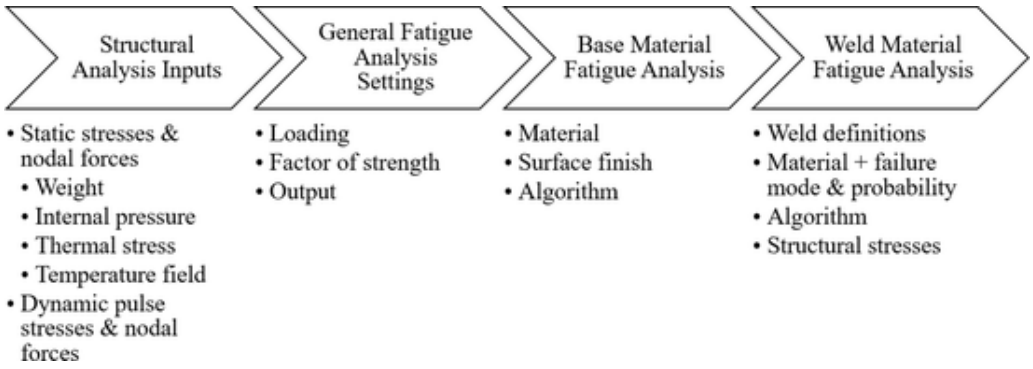

Fig. 12. Fatigue analysis high-level workflow with inputs.

Table 2
Load cases assessed in fatigue analysis.

Load case	Nominal	Up	Down	Over	Under	Side	280 RPM pump speed	350 RPM pump speed	GL[a]
Beam position	Center, normal focus	+6 mm vertical shift	−6 mm vertical shift	Center, over-focused	Center, under-focused	4 mm horiz. shift	Center, normal focus	Center, normal focus	Center, normal focus
Pump speed	400 RPM	400 RPM	400 RPM	400 RPM	400 RPM	400 RPM	280 RPM	350 RPM	400 RPM

[a] GL: hypothesized gas layer condition at the top of the return flow in the target.

minimum life is taken as the fatigue life for that weld. For both types of welds, each of the potential weld failure paths is assigned a weld material S–N curve according to whether it is a weld toe or root/throat failure path. The fatigue algorithm is selected as the worst of the normal or the shear stress. At the time of conducting the analysis, a structural stress weld fatigue life calculation based on the combination of normal and shear stress damage was not available in the software; however, more recent versions of the software include this capability.

4.1. Loading

The fe-safe software can use block loading to evaluate cycles from thermal and pulse loads independently or in combination. Constant static and thermal stresses that act as mean stresses can be included. Table 3 illustrates block loading patterns for evaluating the target module to a design life of 3125 thermal/270M pulse cycles.
The "cycle on/off" pulse loading is an application of the entire pulse stress history per loading cycle. The "Thermal + Pulse" evaluation applies a thermal cycle every 86,400 pulse cycles for a total of 3125 thermal cycles in a 270M cycle period. The first "cold" block applies the static stress superimposed with all pulse stress increments. The second "warm" block applies the static and thermal stress superimposed with all pulse stress increments for 86,400 repeats. The thermal cycling is combined with the pulse cycles so that the combined fatigue damage is automatically calculated. The thermal stress is included in the second block because the target warms up rapidly (within minutes) after receiving the pulsed proton beam; therefore, the target is in a "warm" state for practically all the pulse loading duration. The loading combination of the two blocks is equivalent to 1 repeat in terms of the factor-of-strength (FOS) calculation and life (repeats) output. This approach is explained further in the following section and in the results.

Table 3
Representative block loading patterns for base and weld material evaluated for a design life of 3125 thermal/270M pulse cycles.

Loads/Evaluation	Thermal	Pulse	Thermal + Pulse
Gravity + Pressure	1	1	1
Thermal	1/0	0	1/0 (every 86,400 pulses)
Pulse	0	1/0	1/0
1 = constant on, 0 = constant off, 1/0 = cycle on/off			

4.2. Factor-of-strength calculation

The software calculates an FOS, which is a scalar value by which the loading could be increased or should be decreased to achieve a user-defined design life. The FOS design life is defined as repeats of the entire loading history; therefore, 3125 "repeats" is equivalent to 3125 thermal and 270M pulse cycles. The FOS value is interpreted as a percentage of strain reduction needed to meet the design goal, which is equated to the percentage of strain reduction from gas injection. The current pulse simulation method represents the behavior of the target without gas injection, so this approach is used to evaluate targets that will be operated with gas injection.

4.3. Material properties and fatigue algorithms

The material properties for the 316L stainless-steel base material are derived from the fe-safe material database. Two values in the base material properties are changed from the default values: (1) the constant amplitude endurance limit is changed from 2E7 to 2E10 reversals (2 reversals = 1 cycle) to extend past 1 year of target operation (1.08×10^9 cycles), and (2) a surface finish factor, K_t ~1.06 (stress concentration factor) is selected to represent the range of as-manufactured surface finishes, $0.6 < R_a \leq 1.6$ μm (or $24 < R_a \leq 63$ μ inch), in low-life regions of the nose and front body.
The default and recommended fatigue algorithm for the 316L stainless steel material (and most ductile metals) is the Brown–Miller [15,16]

Table 4
Estimated minimum cycles to thermal fatigue failure for front body base material from normal operation load cases.

Case:	Goal	Nom.	Up	Down	Over	Under	Side	JF 1.4 MW	JF 2 MW
Life:	3125	7.9M	0.76M	0.45M	16M	3.3M	9.7M	6.7M	1.0M

Table 5
Estimated minimum cycles to thermal fatigue failure for weld material from normal operation load cases.

Case:	Goal	Nominal	Up	Down	Over	Under	Side	JF 1.4 MW	JF 2 MW
Life:	3125	63k	61k	66k	63k	63k	120k	200k	80k

Table 6
Estimated minimum cycles to combined thermal and pulse fatigue failure for base material in swirl bubbler for normal operation load cases.

	Goal	Nominal	Up	Down	Over	Under	Side	JF 1.4 MW	JF 2 MW
Bubbler life:	270M	3.1M	4.9M	2.9M	1.4M	10M	No model	N/A	N/A
Required strain reduction	0%	37%	33%	38%	44%	29%	No model	N/A	N/A

combined strain criterion with the Morrow mean stress correction [17]. The Brown–Miller criterion is a multi-axial strain–life algorithm that proposes that the maximum fatigue damage occurs on the plane of maximum shear strain, because cracks tend to initiate on these planes. The fatigue damage is a function of this shear strain and the strain normal to this shear. This plane is identified using the critical plane analysis technique at each material point, and damage accumulates independently for each point. The reported repetitions to failure are the number of loading repetitions necessary to initiate a macroscopic fatigue crack (usually on the order of 1 mm).

The fe-safe/Verity material database contains the master S–N curves that are associated with two material types (steels and aluminums) and two failure modes (toe and root/throat). Detailed descriptions of these curves with equation forms are found in Annex 3-F.2 of the ASME BPVC Sec. VIII Div. 2. Weld fatigue is dominated by stress concentrations, residual stress, and defects. Whereas the residual stress and defects can be inherently accounted for in empirically based fatigue material properties, the stress concentration is varying and difficult to resolve in a finite element model. The structural stress method [11] circumvents this difficulty by using a fatigue driving parameter that is based on a function of linearized membrane and bending stresses along a potential weld failure plane. This is the structural stress parameter, and it is directly calculated from a line balance of nodal forces and moments in an FEA model into work-equivalent tractions. A master curve is then used to query the life corresponding to a structural stress value, much like a traditional S–N fatigue calculation for base material. Because welds contain inherent surface defects and micro-cracking, the reported repetitions to failure are the number of loading repeats necessary to generate a through crack along the specified weld line and failure path.

5. Results and discussion

The following list contains general formatting and guidelines that are used for the interpretation of the results:

- All fatigue contour plots use a log $_{10}$ scale and range from 0 to 3.495 ($10^{3.495} = 3125$ loading repeats = 3125 thermal cycles + 270M pulse cycles).
- PPU results are compared with a result that represents a JF target design operating at 1.4 MW (current operational load) and 2 MW (PPU equivalent load). The JF model is prepared in the same manner as the PPU model.
- For combined thermal and pulse fatigue life, locations with an estimated life of less than the 270M cycle goal are reported with a percentage of strain reduction needed from gas injection.
- The 'Side' case lacks loading symmetry about the center of the target, so a full mercury vessel model is required; it is a less detailed model for computational efficiency.

5.1. Thermal fatigue life

Thermal fatigue life predictions for previous target designs have all exceeded the design criteria, and this pattern continues with the PPU 2 MW target design. Table 4 summarizes the estimated minimum cycles to thermal fatigue failure for the front body base material from various load cases under normal operation, with JF design comparisons for the nominal case included. The order of magnitude decrease for the Up and Down cases corresponds with the increased beam heating of the upper and lower regions of the front body, respectively. Likewise, the Over and Under cases have an approximately 2× increase and 0.5× decrease in minimum life, respectively, because of less and more heating toward the sides of the front body. The Side case result is interesting because it is slightly higher than the Nominal case, indicating that there may be little effect from shifting the beam horizontally.

The minimum weld material thermal fatigue life occurs in the root of the transition to manifold weld near the symmetry plane. Table 5 summarizes the estimated minimum cycles to thermal fatigue failure for normal operation load cases, with JF design comparisons for the nominal case included. The life in the transition weld is driven by the thermal gradients in the rear section of the target, which appear to be minimally affected by the beam position shifts and focusing.

5.2. Combined thermal and pulse fatigue life

Pulse life predictions for past target designs (which operated at 1.4 MW or less) have all been less than the design goals, and this continues to be the case for the PPU 2 MW target design. However, experience shows that targets in operation have survived significantly longer than these predictions, so relative comparisons between target designs are used in the fatigue goals.

The swirl bubbler contains local regions with predicted lives well below 270M cycles, as shown in the contour plot in Fig. 13. No SNS targets operated to date have contained a swirl bubbler, so there is no JF comparison for this region. The life contour plots for the upstream face (left image) and downstream face (right image) of the swirl bubbler are shown in Fig. 13 for the Nominal load case. Required strain reductions from gas injection to reach 270M cycles are also indicated in result plots by the '%' values accompanying the highlighted locations of fatigue life.

All other normal operation load cases except the Up case had minimum life locations in the same area as the Nominal case. The life and strain reductions for the swirl bubbler are summarized in Table 6. The minimum life is 1.4M cycles with a 44% required strain reduction to reach 270M cycles. This magnitude of strain reduction is achievable with gas injection, as past target strain measurements show an average strain reduction from 37 to 50% [18] and more recent measurements range from 30 to 60%. Regardless of the level of conservatism in the fatigue life prediction, it is expected that strain reduction from gas injection will allow the swirl bubbler to meet the 270M cycle design goal; however, the authors also recognize that inaccuracy in the underlying pulse stress prediction may have a detrimental effect on life prediction accuracy.

The front body is the region containing the largest number of locations with life predictions below 270M cycles. Fig. 14 shows these locations for the Nominal case, rank ordered from 1 through 10 by lowest life and highest required strain reduction. The '(#)' location identifier is used to compare similar low life locations between the PPU and JF designs. A similar view with the locations identified for the JF 1.4 MW result is shown in Fig. 15.

The removal of the center baffle from the front body in the PPU design (among other design improvements) creates a different pattern and a smaller number of locations with minimum lives <270M cycles. The minimum life for the PPU design is approximately 5 times larger than that for the JF 2 MW life (not shown), and the number of locations under 270M cycles is 40% less.

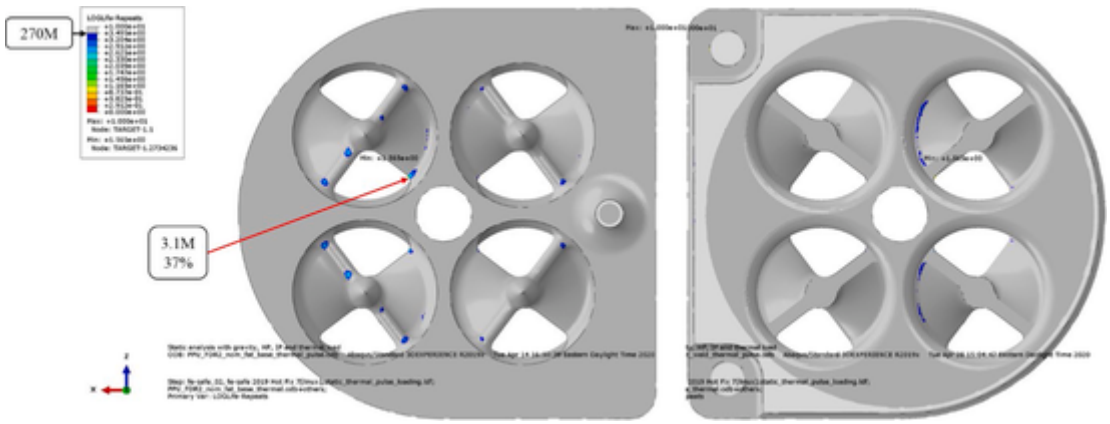

Fig. 13. Estimated minimum cycles to combined thermal and pulse fatigue failure for base material in swirl bubbler for nominal load case. The upstream face (facing incoming mercury flow) is shown on the left and the downstream face (facing incoming beam) is shown on the right.

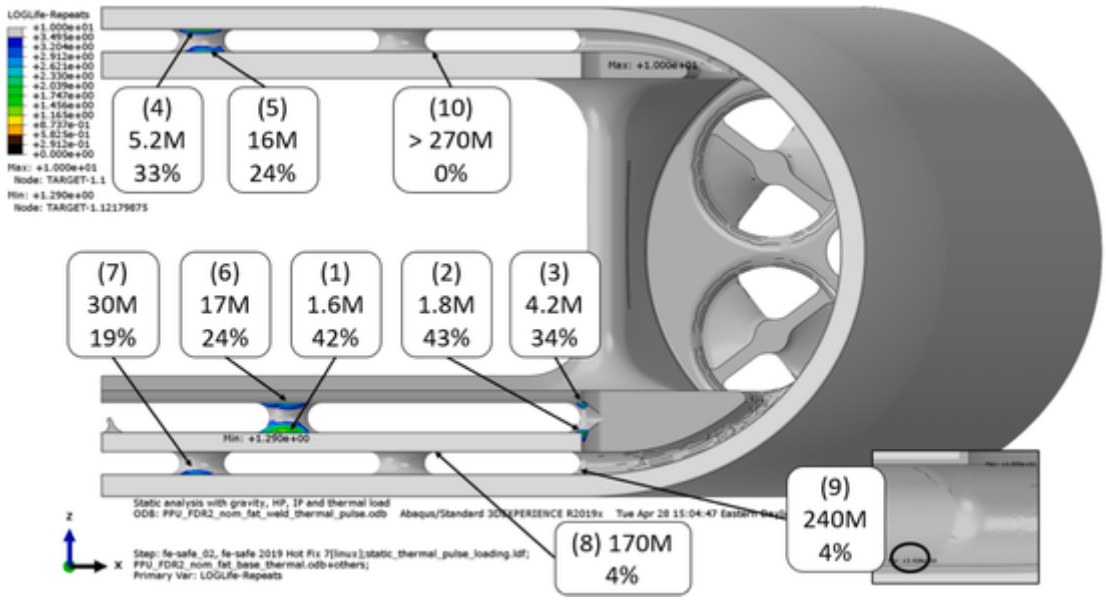

Fig. 14. Estimated minimum cycles to combined thermal and pulse fatigue failure for base material in the front body of the PPU 2 MW target design for the nominal load case. Locations are rank ordered from 1 through 10 by the lowest life/highest required strain reduction (1) to achieve 270M cycles.

The weld material combined thermal and pulse fatigue life is reported in a similar manner to that of the base material; the contour plot for the Nominal case is shown in Fig. 16. Like the base material, the predictions are conservative and fall below the 270M cycle goal. Each weld in the Nominal case meets the design goal of 0.5 times the minimum life in the JF result, or more. The JF 1.4 MW weld results are shown in Fig. 17. The PPU design at 2 MW performs as well as or significantly better than the JF model at 1.4 MW and 2 MW.

5.3. Abnormal operation load cases

The abnormal operation load cases differ from the nominal load case only in the internal pressure and thermal load, and all the cases exceed the fatigue design goal for base and weld material thermal fatigue. Most of the hotspot locations (see Fig. 14) for base material combined fatigue life are unaffected by the abnormal operation load cases. The few locations that do have a significant change in life do not drop below the minimum fatigue life result. The largest change is on the bottom of the window flow return inner rib, location 5 in Fig. 14, which drops from approximately 16M (Nominal) to 2.7M in the GL case (i.e., a hypothesized gas layer condition at the top of the return flow in the target). This result is due to the increased temperature and its gradient caused by the hypothesis that the gas layer is fully insulating. The gas layer could not completely insulate the heat transfer from steel to mercury on the upper surface of the target return flow, so the impact is exaggerated and its effect on fatigue life is conservative. Finally, there is negligible effect from the abnormal operation load cases on weld fatigue life for all load cases.

6. Conclusions

The purpose of this work is to show that the combined design, simulation, and analysis efforts for the PPU 2 MW target have culminated in a design that is predicted to have superior resistance to fatigue failure compared with past designs. The fatigue evaluation used the latest commercially available fatigue analysis software and methods for base and weld material, and it incorporated energy deposition, temperature, and stresses from accelerator physics, neutronics, CFD, and structural simulations. The predicted PPU target fatigue life at 2 MW is comparable to the JF target at 1.4 MW and far exceeds the predicted life of the JF target at 2 MW. Table 7 summarizes the minimum fatigue life results for the PPU and JF target designs.

All cases greatly exceeded the required 3125 thermal cycles. The PPU design met the goal of a minimum combined fatigue life that was at

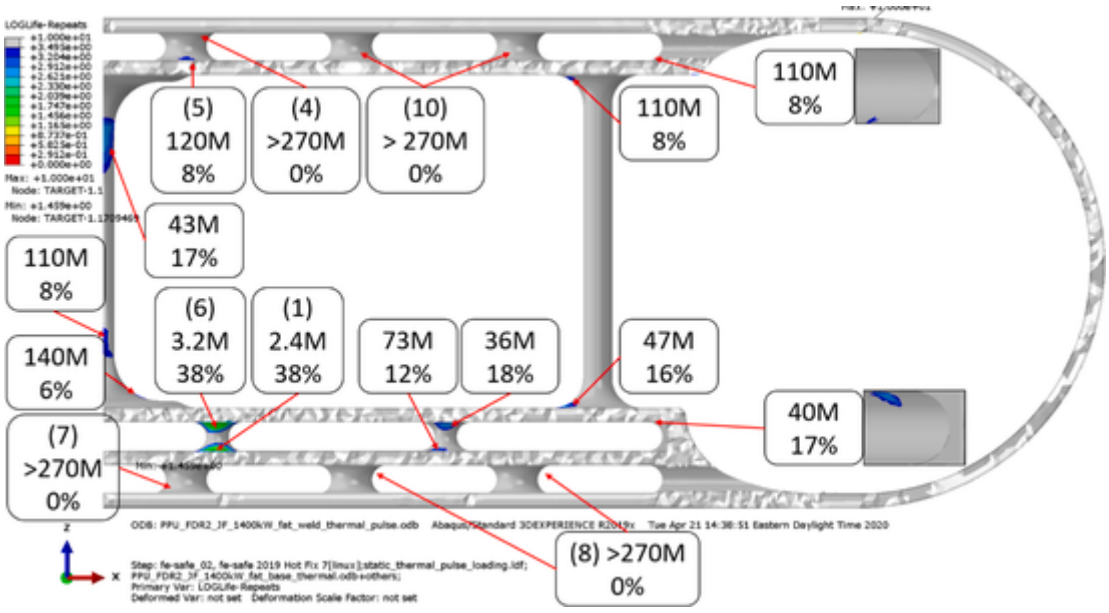

Fig. 15. Estimated minimum cycles to combined thermal and pulse fatigue failure for base material in the front body of the JF 1.4 MW target design for the nominal load case. Locations are rank ordered from 1 through 10 for comparison with the PPU 2 MW target design result (cf. Fig. 14).

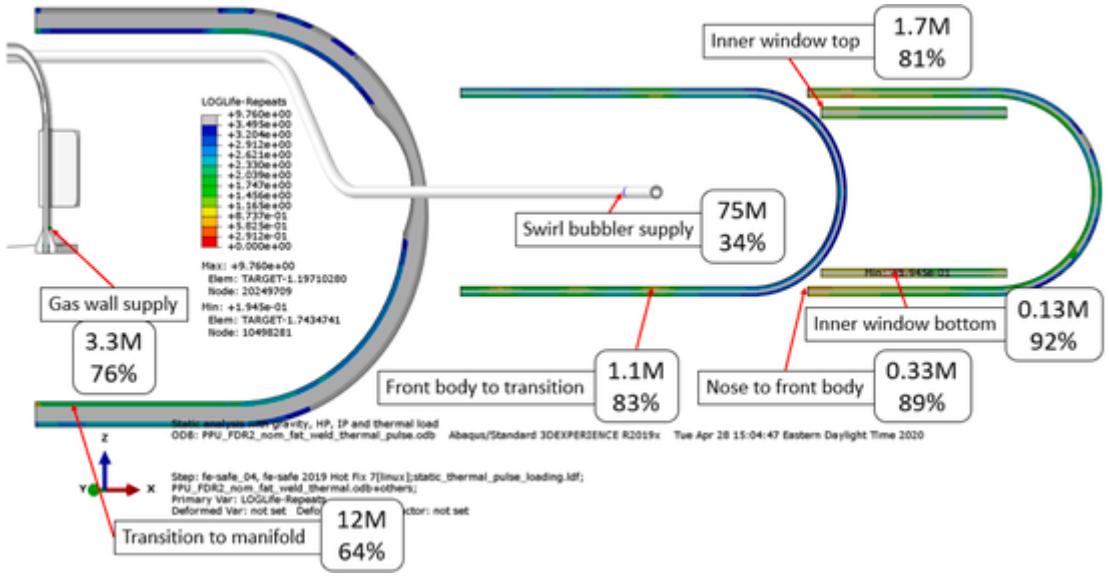

Fig. 16. Estimated minimum cycles to combined thermal and pulse fatigue failure for weld material in the PPU 2 MW target design for the nominal load case.

least 0.5 times the JF 1.4 MW minimum life. Additionally, the minimum combined life was five times greater than the JF 2 MW result. All PPU load cases had a maximum required strain reduction percentage from gas injection that was less than 50% (for base material to reach 270M cycles). It is important to note that measurements of strain reduction from gas injection can (currently) only be taken from the outer surface of the mercury vessel, and that the lowest life regions are on the inner surface (wetted mercury) side of the vessel. This is a limitation that hinders direct comparison of the required and measured strain reductions from gas injection, however, the current measurement trends indicate that increasing levels of gas injection continue to increase the measured strain reductions at the front outer surface of the target (near the lowest life regions). The PPU project will provide the capability for more than 10 times the level of gas injection achieved in current operating targets. This ongoing evaluation of operating JF targets (and increasing gas injection) provides the authors with confidence that the PPU 2 MW target will achieve its lifetime goals. Overall, in this fatigue life assessment, the PPU 2 MW target design showed superior resistance to fatigue failure compared with past target designs.

CRediT authorship contribution statement

Justin Mach: Conceptualization, Methodology, Validation, Formal analysis, Writing - original draft, Visualization. **Kevin Johns:** Conceptualization, Validation, Supervision, Project administration, Writing - review & editing. **Sarma Gorti:** Methodology, Formal analysis, Writing - review & editing. **Hao Jiang:** Methodology, Formal analysis, Writing - review & editing.

Declaration of Competing Interest

The authors declare that they have no known competing financial interests or personal relationships that could have appeared to influence the work reported in this paper.

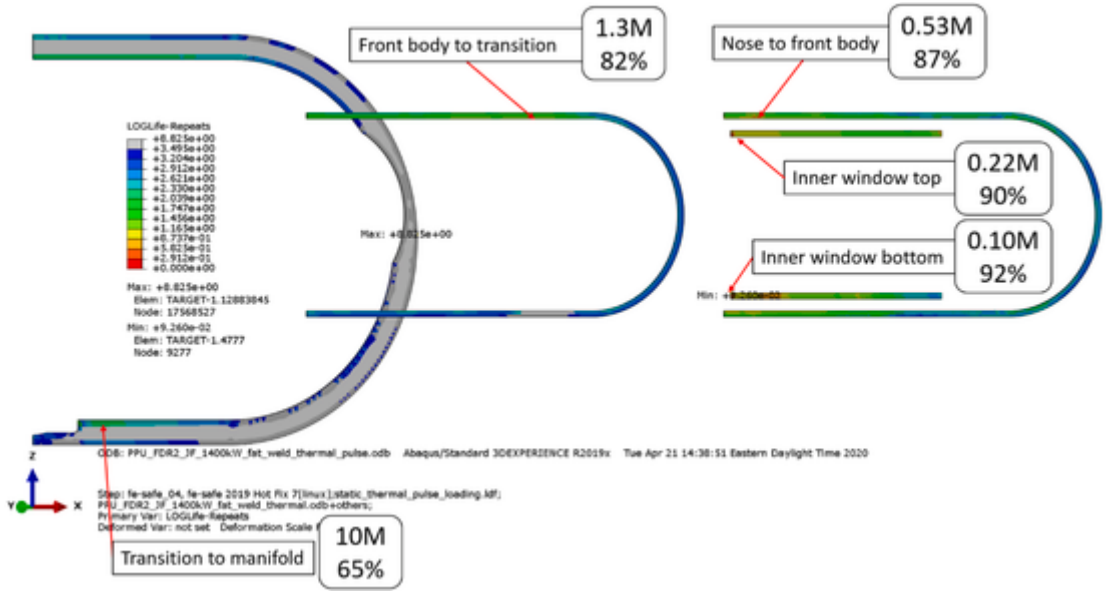

Fig. 17. Estimated minimum cycles to combined thermal and pulse fatigue failure for weld material in the JF 1.4 MW target design for the nominal load case.

Table 7
Summary of minimum fatigue life results.

Load case description	Base material min. thermal life	Base material min. combined life	Base material max. % strain reduction	Weld material min. thermal life	Weld material min. combined life	Weld material max. % strain reduction
JF 1.4 MW	6.7M	2.4M	38%	200k	0.10M	92%
JF 2 MW	1.0M	0.31M	53%	80k	~0	~100%
Nominal	7.9M	1.6M	43%	63k	0.13M	92%
Up	0.76M	0.96M	48%	61k	0.12M	92%
Down	0.45M	1.4M	40%	66k	0.14M	92%
Over	16M	1.0M	46%	63k	0.11M	92%
Under	3.3M	3.0M	37%	63k	0.16M	91%
Side	9.7M	1.5M	41%	120k	0.28M	89%
280 RPM	0.23M	1.4M	44%	23k	0.12M	92%
350 RPM	2.9M	1.4M	45%	50k	0.13M	92%
GL	0.19M	2.0M	38%	66k	0.14M	91%

Acknowledgments

ORNL is managed by UT-Battelle LLC under contract DE-AC05-00OR22725 for the US Department of Energy. This research was supported by the DOE Office of Science, Basic Energy Sciences, Scientific User Facilities.

The authors thank Deborah Counce, Bernie Riemer, Drew Winder, and Mark Wendel for their reviews of this work and Eric Vidal and David McClintock for providing the X-ray and micrograph images, respectively, of the welds.

References

[1] J.R. Haines, T.J. McManamy, T.A. Gabriel, R.E. Battle, K.K. Chipley, J.A. Crabtree, L.L. Jacobs, D.C. Lousteau, M.J. Rennich, B.W. Riemer, Spallation neutron source target station design, development, and commissioning, Nucl. Instrum. Methods Phys. Res. A 764 (2014) 94–115.
[2] J. Galambos, M. Champion, M. Connell, M. Howell, S. Kim, J. Moss, M. Plum, B. Riemer, W. Steffey, K. White, Status of the SNS proton power upgrade project, 29th Linear Accelerator Conf.(LINAC'18), Beijing, China, 16-21 September 2018, JACOW Publishing, Geneva, Switzerland, 2019, pp. 24–28.
[3] M. Howell, B. DeGraff, J. Galambos, S.H. Kim, SNS proton power upgrade, IOP Conf. Ser.: Mater. Sci. Eng. 278 (2017) 012185.
[4] H. Kogawa, M. Futakawa, S. Ishikura, Dynamic response of mercury subjected to pressure wave, J. Nucl. Sci. Technol. 44 (2007) 523–529.
[5] M. Futakawa, T. Naoe, C.C. Tsai, H. Kogawa, S. Ishikura, Y. Ikeda, H. Soyama, H. Date, Pitting damage by pressure waves in a mercury target, J. Nucl. Mater. 343 (2005) 70–80.
[6] VIII rules for construction of pressure vessels, division 2, alternative rules, 2019 ASME Boiler & Pressure Vessel Code, ASME International, New York, NY, 2019.
[7] J.P. Strizak, H. Tian, P.K. Liaw, L.K. Mansur, Fatigue properties of type 316LN stainless steel in air and mercury, J. Nucl. Mater. 343 (2005) 134–144.
[8] T. Naoe, Z. Xiong, M. Futakawa, Gigacycle fatigue behaviour of austenitic stainless steels used for mercury target vessels, J. Nucl. Mater. 468 (2016) 331–338.
[9] B.W. Riemer, Benchmarking dynamic strain predictions of pulsed mercury spallation target vessels, J. Nucl. Mater. 343 (2005) 81–91.
[10] B. Riemer, J. Haines, D. Lousteau, T. McManamy, Thermal shock simulations of the sns mercury target module using Abaqus/Explicit, in: Proc. of the Third International Meeting of Nuclear Applications in Accelerator Technology (AccApp '99), Long Beach, California, 1999.
[11] P. Dong, J. Hong, A robust structural stress parameter for evaluation of multiaxial fatigue of weldments, J. ASTM Int. 3 (2006) 1–17.
[12] M. Ida, T. Naoe, M. Futakawa, On the effect of microbubble injection on cavitation bubble dynamics in liquid mercury, Nucl. Instrum. Methods Phys. Res. A 600 (2009) 367–375.
[13] C. Barbier, E. Dominguez-Ontiveros, R.L. Sangrey, Small bubbles generation with swirl bubblers for SNS target, in: 5th Joint US-European Fluids Engineering Summer Conference, Montreal, Quebec, Canada, 2018.
[14] H. Kogawa, T. Naoe, T. Wakui, K. Haga, M. Futakawa, H. Takada, Pressure wave reduction due to gas microbubbles injection in mercury target of J-PARC, International Collaboration on Advanced Neutron Sources (ICANS-21), Mito, Japan, 2015, pp. 70–75.
[15] F.A. Kandil, M.W. Brown, K. Miller, Biaxial low-cycle fatigue failure of 316 stainless steel at elevated temperatures, Mechanical Behaviour and Nuclear Applications of Stainless Steel at Elevated Temperatures, 1982.
[16] M.W. Brown, K. Miller, A theory for fatigue failure under multiaxial stress–strain conditions, Proc. Inst. Mech. Eng. 187 (1973) 745–755.
[17] J. Morrow, in: J. Graham (Ed.), Fatigue Design Handbook, Society of Automotive Engineers, New York, 1968, pp. 21–29.
[18] Y. Liu, W. Blokland, C. Long, S. Murray III, B. Riemer, R. Sangrey, M. Wendel, D. Winder, Strain measurement in the recent SNS mercury target with gas injection, J. Phys. Conf. Ser. (2018).